Journal of FISH BIOLOGY

fsbi An International Society for Fish Biology

Journal of Fish Biology (2017) **90**, 1338–1355
doi:10.1111/jfb.13240, available online at wileyonlinelibrary.com

Reconstructing larval growth and habitat use in an amphidromous goby using otolith increments and microchemistry

J. D. Hogan*†, R. Kozdon‡§, M. J. Blum§, J. F. Gilliam‖, J. W. Valley‡ and P. B. McIntyre¶

*Department of Life Sciences, Texas A&M University – Corpus Christi, 6300 Ocean Drive, Unit 5892, Corpus Christi, TX 78412, U.S.A., ‡WiscSIMS, Department of Geoscience, University of Wisconsin – Madison, 1215 W. Dayton St, Madison, WI 53706, U.S.A., §Department of Ecology and Evolutionary Biology, Tulane University, 400 Lindy Boggs Building, New Orleans, LA 70118, U.S.A., ‖Department of Biology, North Carolina State University, Raleigh, NC 27695, U.S.A. and ¶Center for Limnology, University of Wisconsin – Madison, 680 N. Park St, Madison, WI 53706, U.S.A.

(Received 20 January 2016, Accepted 4 November 2016)

High-resolution analysis of growth increments, trace element chemistry and oxygen isotope ratios ($\delta^{18}O$) in otoliths were combined to assess larval and post-larval habitat use and growth of *Awaous stamineus*, an amphidromous goby native to Hawai'i. Otolith increment widths indicate that all individuals experience a brief period of rapid growth during early life as larvae and that the duration of this growth anomaly is negatively correlated with larval duration. A protracted high-growth period early in larval life is associated with a lower ratio of Sr:Ca, which may reflect low salinity conditions in nearshore habitats. A distinct shift in $\delta^{18}O$ (range: 4–5‰) is closely associated with the metamorphic mark in otoliths, indicating that larval metamorphosis occurs promptly upon return to fresh water. Strontium and other trace elements are not as tightly coupled to the metamorphosis mark, but confirm the marine-to-freshwater transition. Integration of microstructural and microchemical approaches reveals that larvae vary substantially in growth rate, possibly in association with habitat differences. Although time and financial costs make it difficult to achieve large sample sizes, present results show that examining even a small number of individuals can lead to novel inferences about early life history in diadromous fishes and illustrates the value of integrating analyses.

Key words: *Awaous stamineus*; LA-ICP-MS; migration; otolith ageing; SIMS; Sr:Ca.

INTRODUCTION

Although information on early life history remains elusive for most fishes, it is becoming clear that individual variation in larval fish habitat use can influence survival and demography (Hogan *et al.*, 2014). The environment that larvae experience can greatly

†Author to whom correspondence should be addressed. Tel.: +1 361 825 5883; email: james.hogan@tamucc.edu
§Present address: Lamont–Doherty Earth Observatory of Columbia University, 61 Route 9W, Palisades, NY 10964, U.S.A.

influence growth rate (Grorud-Colvert & Sponaugle, 2011; Hogan *et al.*, 2014) and condition upon settlement (Hamilton *et al.*, 2008), which are linked to post-settlement survival (Hamilton *et al.*, 2008; Grorud-Colvert & Sponaugle, 2011) and later reproductive fitness (Weiss *et al.*, 1987). Larval habitat use may also strongly influence recruitment and connectivity among populations, as has been shown for some marine species (Mora & Sale, 2002). It remains challenging, however, to reconstruct habitat use and growth given the small size and mobility of larval fishes.

Otoliths provide an indelible and highly informative record of individual life history, habitat use and growth from hatching to death (Campana, 1999). Otolith microstructures, such as daily or annual growth rings, have long been used as indicators of individual performance including growth rate and longevity, due to the daily deposition of protein and carbonate layers and their strong, positive correlation with somatic growth (Campana, 1999). Information on otolith microstructure has also been coupled with exogenous measurements of environmental variables to understand relationships between environment, growth and survival (Grorud-Colvert & Sponaugle, 2011). The recent advent of tools such as laser-ablation inductively coupled plasma mass spectrometry (LA-ICP-MS) and secondary ion mass spectrometry (SIMS) now affords opportunities to reconstruct retrospective records of habitat use, movement and life-history parameters based on geochemical variation among habitats (Elsdon *et al.*, 2008). Such inferences often reflect shifts in the concentrations of trace elements such as strontium (Sr), barium (Ba), magnesium (Mg) and manganese (Mn) that are rare yet consistently present within the calcium carbonate matrix of otoliths (Campana, 1999).

LA-ICP-MS is one of the most commonly used tools for analysis of otolith microchemistry, particularly of the early life-history stages of fishes (Elsdon *et al.*, 2008). The technique uses a laser to ablate (LA) the surface of the otolith, which volatilizes material that then passes through plasma (ICP). The materials are ionized and then passed into a mass spectrometer (MS), which separates isotopes by mass–charge for determination of the ablated materials composition (Durrant & Ward, 2005). Laser transects can be used to measure elemental composition of an otolith across the growth radius (*i.e.* from core to edge). Most studies of otolith microchemistry during early life stages have focused on Sr and other trace elements, but stable isotopes of oxygen, carbon and other abundant light elements (which cannot be measured by LA-ICP-MS) can lend additional perspective on habitat use and growth.

SIMS is another technique that can be used to analyse the isotopic composition of material surfaces (Valley & Kita, 2009). It uses a focused beam of caesium (Cs) ions (10 μm diameter in this study) to sputter secondary ions of oxygen from the surface of the experimental material, in this case otoliths (Valley & Kita, 2009). The mass:charge ratio of the ions is then measured with a mass spectrometer to determine isotope concentrations of abundant light elements (*i.e.* C and O) in the material (Valley & Kita, 2009). SIMS requires high precision in sample preparation because smooth and even surfaces are required for proper quantification of sputtered secondary ions (Kita *et al.*, 2009). SIMS analysis offers higher spatial resolution of the sampling beam than LA-ICP-MS (Durrant & Ward, 2005), thereby generating higher temporal resolution of oxygen and carbon isotope records. In fishes with fast growing otoliths, SIMS can allow sampling of individual daily growth increments (Weidel *et al.*, 2007). SIMS can also offer a unique perspective on fish habitat use and migration, as patterns of oxygen isotope ratio in otoliths reflect the $\delta^{18}O$ and $\delta^{13}C$ of water and the temperature-dependent fractionation between water and carbonate (Limberg *et al.*, 2013; Matta *et al.*, 2013).

Because light isotopes of oxygen (*i.e.* ^{16}O) evaporate slightly more readily than heavy oxygen (*i.e.* ^{18}O), rainwater is depleted of ^{18}O (Bradley, 1999). Freshwater systems driven by rainfall consequently often exhibit lower ^{18}O:^{16}O (expressed as $\delta^{18}O$) than sea water. Thus, $\delta^{18}O$ can be used as a proxy for the environmental temperature and water sources experienced by a fish at any particular time in its life cycle.

Just 5% of otolith studies have so far merged microstructural and microchemical analyses of otoliths (Starrs *et al.*, 2016), even though integrated analyses can substantially increase inferential power, particularly for understanding early life-history stages (Hamilton *et al.*, 2008; Shima & Swearer, 2009; Hogan *et al.*, 2014). Recent work has shown the value of combining otolith chemistry and microstructure to reconstruct the timing of juvenile Pacific bluefin tuna *Thunnus maccoyii* (Castelnau 1782) migrations (Baumann *et al.*, 2015). Here, three different techniques (microstructural analysis, LA-ICP-MS and SIMS) are combined to examine the migratory, early life history of *Awaous stamineus* (Eydoux & Souleyet 1850), an at-risk facultative amphidromous goby (Hogan *et al.*, 2014) native to the Hawai'ian archipelago (Lindstrom *et al.*, 2012; Walter *et al.*, 2012) that is afforded protection by the State of Hawai'i (www.dlnr.hawaii.gov). To further understand the linkage between individual growth and habitat use of *A. stamineus*, otolith microstructures were used to quantify larval growth rate, trace element microchemistry to determine chemical environments (*e.g.* salinity) experienced during early life history and oxygen isotope ratios to test for temperature or salinity shifts experienced by individual larvae. Focusing on migratory larvae that returned to streams from an offshore environment, all three kinds of data were compared to evaluate the potential benefits of integrative analysis and to infer the influence of habitat on growth performance during early life stages of *A. stamineus*.

MATERIALS AND METHODS

STUDY SPECIES AND FIELD SAMPLING

Awaous stamineus is a stream-dwelling fish that inhabits the lower and middle reaches of perennial streams in the Hawai'ian Islands (Keith, 2003). It is facultatively amphidromous; adults spawn benthic eggs in freshwater streams, newly hatched larvae either remain in fresh water or migrate downstream to estuarine or marine environments and migratory larvae then return to fresh water where most growth and maturation occur during juvenile post-larval and adult stages (Hogan *et al.*, 2014). Eggs hatch after 48 h (Kinzie, 1990). Larvae that migrate downstream to the ocean (McDowall, 2007) spend up to 5 months at sea (Radtke *et al.*, 1988; Hogan *et al.*, 2014). Adults can achieve a size of at least 340 mm, with males and females becoming readily distinguished at *c.* 70 mm (J. D. Hogan, pers. obs.). Individuals live 2·5 years on average (Hogan *et al.*, 2014), most or all of which is spent in fresh water, including maturation and spawning life-history stages. Historically, *A. stamineus* were abundant enough to support an artisanal fishery, but population declines resulting from anthropogenic activities (Brasher, 2003; Walter *et al.*, 2012) have led to a fishing ban (Ha & Kinzie, 1996).

Recruiting post-larvae ($n = 9$) were collected from sites near the mouths of five catchments in the Hawai'ian archipelago including Waimea, Kaluanui and Waimanalo catchments on O'ahu, Lawa'i catchment on Kaua'i and Halawa catchment on Moloka'i. For this study, post-larvae were considered to be newly recruited fishes that have undergone metamorphosis in the stream environment. The total length (L_T) range of specimens was 21–26 mm. The sampled streams are representative of the diversity of land use (forested to urban) and stream water temperatures (21·1–24·5° C at the time of sampling) across the archipelago. Sampling was conducted from April to June 2011. Fish were collected by snorkelers with hand nets, measured for L_T, euthanized and stored frozen.

OTOLITH MICROSTRUCTURE ANALYSES

Detailed age and daily growth data were collected for sagittal otoliths from nine *A. stamineus* post-larvae. Daily increment formation in this and other Hawai'ian amphidromous gobies was validated by Radtke *et al.* (1988), who used EDTA to chelate the $CaCO_3$ structure to reveal well defined bands of protein and scanning electron microscope (SEM) to image the otoliths increments. After fish were thawed, sagittal otoliths were extracted using teflon coated forceps and a fine-bristled paint brush. Otoliths were manually cleared of soft tissue, dried and stored in polypropylene vials. For each fish, one otolith was arbitrarily selected for microstructure analysis of daily growth rings and LA-ICP-MS trace-element chemistry. This otolith was mounted onto a petrographic slide in Crystalbond 509 (www.aremco.com) adhesive, then ground and polished in the sagittal plane using fine-grit (30–3 μm grit size) diamond coated lapping films (3M; www.3m.com) to reveal the daily growth rings from the primordium to the edge. Multiple images of each otolith were taken in different focal planes with a Leica digital camera (www.leica-camera.com) mounted to a compound microscope using a ×20 objective lens and then stitched together in Photoshop (www.adobe.com) to create one image focused on the otolith increments from primordium to edge. Daily growth rings were counted and increment widths were measured along the longest growth axis using Leica application suite software. Otoliths were read in triplicate by a single reader; each reading was done blind to the sample number, with samples randomized between reads. Any otoliths that demonstrated >15% variation between the two closest reads were excluded from further consideration; none of the otoliths here met that criterion and so all were retained for analysis.

Age and daily growth rate before and after metamorphosis were determined based upon a clearly visible metamorphic mark on the otolith characterized by a thick band of high optical density (Radtke *et al.*, 1988). The number of rings from the primordium to the metamorphosis mark was considered to reflect larval duration (in days) and post-larval age was the number of daily rings from the metamorphosis mark to the otolith edge (Radtke *et al.*, 1988). Daily growth was measured for both larval and post-larval growth periods. It was assumed that somatic growth and otolith growth are closely related. Otolith growth and somatic growth, however, can become decoupled during periods of starvation when somatic growth stops while otolith growth continues (Barber & Jenkins, 2001). Daily growth rates declined sharply during the course of the larval period for all individuals, hence periods of above-average daily growth rates were used to differentiate an early larval growth (ELG) period from the slower growth exhibited during the late larval growth (LLG) period. The end of the ELG period was identified as the point when daily growth first dropped below the average for an individual larva. The LLG period was considered to be the remainder of the larval period prior to metamorphosis. The sum of the ELG and LLG represents the total duration of the larval period and size at metamorphosis was considered to be proportional to the length of the radius (LOR) from the primordium to the metamorphic mark along the longest axis. To test whether the duration of the ELG predicts future growth, ELG duration was compared with LLG duration and PLD (in days), size at metamorphosis and post-larval growth rate (PLG).

LA-ICP-MS ANALYSIS

The same otolith used for microstructural analysis was subsequently analysed for trace-element chemistry by laser ablation inductively coupled plasma mass spectrometry (LA-ICP-MS). Otolith samples were triple-rinsed with deionized water and dried. Otoliths were then analysed with a Cetac LSX-213 (laser ablation; www.teledynecetac.com) and PerkinElmer ELAN DRC II (quadrupole inductively coupled plasma mass spectrometer; www.perkinelmer.com) at the Analytical Geochemistry Laboratory at the University of Massachusetts – Boston. Samples were analysed with a laser transect (pulse rate, 20 Hz; energy, 70%; circular beam diameter, 25 μm; scan rate, 15 $\mu m\ s^{-1}$) starting at one edge of the otolith, bisecting the primordium and ending at the other edge of the otolith, resulting in a palindromic signal. Fourteen elements (Mg, Ca, Ti, Cr, Mn, Ni, Cu, Zn, Rb, Sr, Ba, La, Ce and Pb) were analysed sequentially, yielding one measurement of each mass every 1·16 s. The specific isotopes analysed are listed in Table I. All samples were calibrated and drift corrected using two calcium carbonate pressed-powder pellet standards (United States Geological Survey MACS-1

and MACS-3; http://crustal.usgs.gov/geochemical_reference_standards/microanalytical_RM.html/) and background corrected against the argon carrier gas. Concentrations ($\mu g\,l^{-1}$) were calculated for each measurement across the transect using GeoPro software (Cetac). Relative concentrations of all elements were expressed as ratios to Ca. Minimum detection limits (DL) were determined as 3 s.d. of the mean background gas values. The statistical analysis used only isotopes that either were above the DL in most samples or demonstrated palindromic symmetry about the otolith primordium despite values below DL. Ben-Tzvi *et al.* (2007) showed that sub-DL isotopes which show symmetrical signals around the primordium are highly unlikely be spurious and therefore represent valid data for further analysis. Palindrome analysis was conducted following the procedure outlined in Hogan *et al.* (2014). Four elements (Ca, Sr, Ba and Mg) were consistently above detection limits in most samples and seven more (Mn, Cr, Ni, Cu, Zn, La and Pb) were below detection limits, but demonstrated palindromic symmetry about the origin.

Concentrations of the 11 elements were calculated in the otoliths of each *A. stamineus* individual. To determine changes in habitat use, Sr:Ca was relied on as an indication of salinity (Zimmerman, 2005), which is expected to change markedly as migratory larvae return to freshwater streams from the estuarine or marine environment. Multivariate analysis of variance (MANOVA) was used to test for differences in multi-element chemistry (from LA-ICP-MS) between the pre-metamorphosis period and the post-metamorphosis period. Sr:Ca was compared with the location of the metamorphosis mark to test the interpretation that metamorphosis coincides with the transition to fresh water. Furthermore, MANOVA of all 10 element:Ca ratios was used to test whether the ELG and LLG periods occur in the same environment and regression analysis was used to determine whether ELG duration reflected habitat-use patterns. Levene's test for homogeneity of variances was used to confirm that the data conform to MANOVA assumptions. All statistical analyses were performed in Statistica 13.1 (StatSoft; www.stasoft.com).

OXYGEN ISOTOPE RATIOS BY SECONDARY ION MASS SPECTROMETRY (SIMS)

The second sagittal otolith from each individual was used for oxygen isotope analysis. It was roasted in a vacuum oven at 262° C for 2 h to remove protein and other organic materials prior to sectioning and polishing. Each roasted otolith was mounted in EpoxiCure epoxy resin (Buehler; www.buehler.com) on a glass coverslip with the sulcus facing upward away from the glass. A grain of UWC-3 calcite standard [$\delta^{18}O = 12{\cdot}49‰$ Vienna standard mean ocean water (VSMOW); Kozdon *et al.*, 2009] was mounted adjacent to the otolith. Once hardened, the mounted otolith and standard were embedded facing downward in a 25·4 mm epoxy round (*i.e.* the glass coverslip was at the surface of the round). The epoxy rounds were ground down with 6 μm diamonds embedded in a Buehler wheel until the glass covering the otolith and standard were ground away. Samples were then polished with fine-grit diamond slurries (range: 3·0–0·05 μm) to ensure that the entire growth surface was exposed from primordium to edge and to ensure a flat and smooth sampling surface (vertical tolerance < 5 μm) as determined using an optical surface profilometer (Kita *et al.*, 2009). Epoxy rounds with samples and standards were triple rinsed with distilled water and ethanol, and excess moisture was removed with compressed purified nitrogen gas. Mounts were dried several hours in a vacuum oven at *c.* 40° C and then gold coated for SIMS analysis. Oxygen isotopes and hydroxide (^{16}OH) anions were measured by CAMECA-IMS-1280 ion microprobe (www.cameca.com) at the WiscSIMS Laboratory at the University of Wisconsin – Madison. The primary ion beam was $^{133}Cs^+$ at 1·3 nA. Each analysis took *c.* 3·5 min and a series of spot samples were made for each otolith ($n = 13–18$ spots per fish). Sample spots were ovoid with a length of *c.* 15 μm, width of *c.* 10 μm and depth of *c.* 1 μm [verified by SEM imagery; Figs S1 and S2 (Supporting Information)]. SIMS spots were analysed across the otolith surface along a transect from primordium to edge along the longest axis. Ions were extracted with 10 kV and selected using a 40 eV energy window. Multiple Faraday cups were used to simultaneously measure ^{18}O, ^{16}O and ^{16}OH. Four measurements calcite standards (UWC-3) were made after every *c.* eight sample spots to correct otolith data for instrumental mass bias and drift.

Sample roasting only partially eliminated the organic content of otoliths, as indicated by measurements of the ^{16}OH peak during sample analyses. This remaining organic

TABLE I. Summary of post-larval (stream) chemistry for nine *Awaous stamineus* from five catchments (with water temperature measured at the time of sample collection) across the Hawai'ian Archipelago. All values are the average post-larval measurements from LA-ICP-MS or SIMS. Mean within-catchment values are presented for catchments with multiple individuals

Sample	Island	Catchment	Mg:Ca	Cr:Ca	Mn:Ca	Ni:Ca	Cu:Ca	Zn:Ca	Sr:Ca	Ba:Ca	La:Ca	Pb:Ca	$\delta^{18}O$	° C
10166	Moloka'i	Halawa	0·18*	0·07*	0·48*	0·02*	0·06*	0·06*	143·89	0·27*	0·04*	0·01*	n/a	21·1
10910	Kaua'i	Lawa'i	0·21	0·04*	1·57*	0·21*	0·13	0·10*	255·30	0·33*	0·00*	0·01	n/a	22·7
10912	Kaua'i	Lawa'i	0·18	0·04*	1·48*	0·05*	0·01*	0·06*	84·07	0·69	0·04	0·01*	n/a	22·7
10918	Kaua'i	Lawa'i	0·35	0·09*	3·35	0·15*	0·38*	0·09*	121·59	0·56	0·01	0·01	23·51	22·7
10919	Kaua'i	Lawa'i	0·32*	0·03*	1·49*	0·02*	0·31*	0·33*	100·34	0·69*	0·02*	0·03*	n/a	22·7
Mean	Kaua'i	Lawa'i	0·26	0·05	1·97	0·11	0·20	0·14	140·32	0·57	0·02	0·01	23·51	22·7
11455	O'ahu	Waimanalo	0·15	0·02*	0·00*	0·19*	0·24*	0·20*	39·92	0·25	0·04*	0·07*	22·45	24·5
11527	O'ahu	Kaluanui	0·08	0·01*	0·09*	0·06*	0·10*	0·02*	49·34	0·10	0·01	0·01	23·60	22·5
11542	O'ahu	Waimea	0·09	0·01*	0·00*	0·06*	0·07*	0·03*	94·84	0·09*	0·01*	0·01*	23·15	24·3
11543	O'ahu	Waimea	0·10	0·10*	4·04	0·08*	0·15*	0·28*	177·86	1·10	0·06*	0·11*	23·87	24·3
Mean	O'ahu	Waimea	0·09	0·06	2·02	0·07	0·11	0·15	136·35	0·60	0·03	0·06	23·27	24·3
		Mean	0·19	0·05	1·45	0·09	0·16	0·13	120·75	0·47	0·02	0·03	23·37	23·1
		C.V.	0·47	0·64	0·88	0·67	0·66	0·74	0·48	0·62	0·67	1·33	0·02	0·05

*Values below detection limits are indicated.

material may potentially shift $\delta^{18}O$ analyses to lower values. The effect on analytical precision is negligible, but accuracy within the spot-to-spot reproducibility on standard grains (±0·3‰, 2 S.D., on bracketing standards) cannot be guaranteed. Therefore, oxygen isotope values were corrected for instrumental drift, (notation: $\delta^{18}O_{\text{drift corrected}}$), but not further converted to the VSMOW or pee-dee belemnite scale, as these scales imply accuracy. $\delta^{18}O$ profiles were only interpretable for five of the nine individuals due to inadvertent over or under-grinding of the otolith during preparation, causing data to not reflect the entire life of the fish [raw data for all samples are provided in Table SI (Supporting Information)].

Values of $\delta^{18}O$ are lower in fresh water than in the ocean, so $\delta^{18}O$ was used as a second indicator of larval transition from marine to freshwater habitats around metamorphosis. The relative precision of $\delta^{18}O$ *v.* Sr:Ca as an indicator of this habitat transition was compared with respect to the location of the metamorphic mark. Shifts in $\delta^{18}O$ within the larval and post-larval periods, which could be interpreted as changes in temperature or salinity, were also investigated.

RESULTS

AGE AND GROWTH

The average age of the nine individuals examined was 153 days (range: 132–165 days; C.V. = 0·08; Table II) and the average larval duration was 120 days (range: 105–135 days; C.V. = 0·08; Table II). The sampled individuals exhibited considerable variation in otolith size at metamorphosis (from primordium to metamorphic mark; mean: 231 μm; range: 145–283 μm; C.V. = 0·19). Post-larval growth (PLG; mean = 3·51 μm day^{-1}) rates were significantly higher than mean larval growth rates (mean = 1·91 μm day^{-1}; $t_{16} = -2{\cdot}94$, $P < 0{\cdot}01$, $n = 9$; Figs 1 and 2). Growth within the larval period, however, was not constant; growth during the ELG period (mean = 3·29 μm day^{-1}) was significantly faster than growth during the LLG period (mean = 1·55 μm day^{-1}; $t_{16} = 12{\cdot}77$, $P < 0{\cdot}01$, $n = 9$; Figs 1 and 2). Interestingly, the ELG growth rate exceeded the PLG rate in some samples, but the mean difference among individuals was not statistically significant ($t_{16} = -0{\cdot}40$, $P > 0{\cdot}05$, $n = 9$; Table II). The duration of the ELG also varied widely among individuals (mean: 28 days; range: 18–39 days; C.V. = 0·22; Table II and Fig. 3).

The ELG duration was strongly negatively correlated with LLG duration (days), the period of larval growth remaining after the early larval growth period ended ($r^2 = 0{\cdot}80$, $P < 0{\cdot}01$, $y = -2{\cdot}16x + 152{\cdot}17$, $n = 9$; Fig. 4). The slope of this relationship is *c.* −2, indicating that 1 day of fast growth in the ELG corresponds to two fewer days of late slow growth in the LLG. As a result, individuals with extended early growth anomalies completed their larval period in a significantly shorter period of time as indicated by the significant negative correlation between ELG duration and total PLD ($r^2 = 0{\cdot}54$, $P < 0{\cdot}05$, $y = -1{\cdot}16x + 152{\cdot}17$, $n = 9$; Fig. 4). The slope of the relationship between larval otolith radius (LOR) and pelagic larval duration (PLD) was 1·8, indicating that the average daily larval growth increment was 1·8 μm ($r^2 = 0{\cdot}17$, $P > 0{\cdot}05$, $y = 1{\cdot}84x + 9{\cdot}90$, $n = 9$). The ELG duration was not related with either size at settlement [larval otolith radius (LOR): $r^2 = 0{\cdot}02$, $P > 0{\cdot}05$, $n = 9$] or post-larval growth rate (PLG: $r^2 = 0{\cdot}06$, $P > 0{\cdot}05$, $n = 9$).

TABLE II. Age and growth statistics for nine *Awaous stamineus* from five catchments across the Hawai'ian Archipelago

Sample	Island	Catchment	Date collected	Hatching date	L_T (mm)	Age (days)	LD (days)	PM (days)	LOR (μm)	MLG (μm day^{-1})	ELG (μm day^{-1})	LLG (μm day^{-1})	ELGD (days)	PLG (μm day^{-1})
10166	Moloka'i	Halawa	23 April 2011	9 November 2010	24	165	123	42	200	1·63	2·66	1·26	32	3·12
10910	Kaua'i	Lawa'i	17 May 2011	6 December 2010	25	162	135	27	225	1·67	3·07	1·48	18	4·19
10912	Kaua'i	Lawa'i	17 May 2011	7 December 2011	24	161	123	38	283	2·12	3·50	1·77	24	2·58
10918	Kaua'i	Lawa'i	17 May 2011	26 December 2010	24	142	111	30	269	2·42	3·68	1·77	39	3·44
10919	Kaua'i	Lawa'i	17 May 2011	30 December 2010	24	138	105	33	145	1·90	3·08	1·45	29	4·39
11455	O'ahu	Waimanalo	2 June 2011	19 December 2010	26	165	111	54	201	1·81	3·05	1·31	32	2·59
11527	O'ahu	Kaluanui	7 June 2011	4 January 2011	21	154	129	25	247	1·91	3·27	1·57	26	2·32
11542	O'ahu	Waimea	8 June 2011	27 January 2011	26	132	118	14	261	2·21	3·62	1·77	28	7·04
11543	O'ahu	Waimea	8 June 2011	3 January 2011	22	156	126	30	249	1·98	3·72	1·59	23	1·92
				Mean	24	153	120	33	231	1·96	3·29	1·55	28	3·51
				C.V.	0·07	0·08	0·08	0·35	0·19	0·13	0·11	0·12	0·22	0·44

ELG, early larval growth rate anomaly; ELGD, early larval growth anomaly duration; L_T, total length; LD, larval duration; LLG, late larval growth rate; LOR, larval otolith radius, used as a proxy for size at metamorphosis; MLG, mean larval growth rate; PLG, post-larval growth rate; PM, post-metamorphosis age.

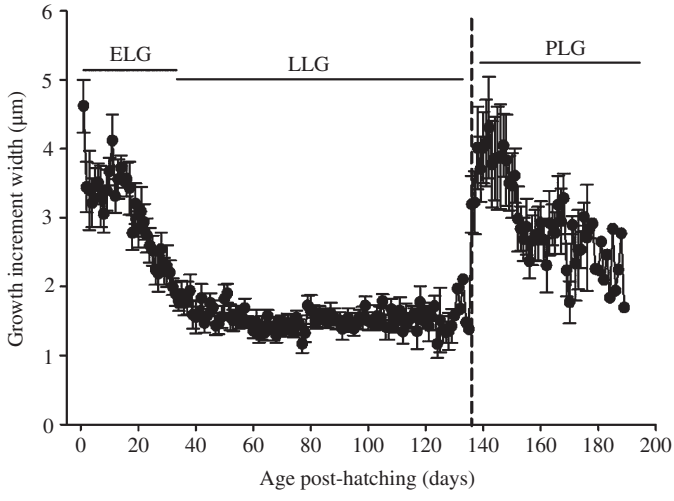

FIG. 1. The mean ± S.D. daily growth profile for nine otoliths from *Awaous stamineus* in the Hawai'ian Archipelago. ELG, the early, fast, larval growth period; LLG, the late, slow, larval growth period; PLG, the post-larval growth period; ●, mean daily growth increments; ⋮, transition from larval to post-larval growth periods.

OTOLITH ELEMENTAL AND ISOTOPIC CHEMISTRY

Multivariate analysis of variance revealed a significant shift in elemental chemistry proximate to the metamorphosis mark in the otoliths (MANOVA: $F_{7,10} = 3{\cdot}70$, $P < 0{\cdot}05$, $n = 9$). Univariate results showed that Sr and Ba were the only elements from LA-ICP-MS to differ significantly between pre- and post-metamorphosis (Sr: $F_{1,16} = 21{\cdot}17$, $P < 0{\cdot}01$, $n = 9$; Ba: $F_{1,16} = 8{\cdot}87$, $P < 0{\cdot}01$, $n = 9$). Both Sr:Ca and $\delta^{18}O$ profiles indicate a major shift in environmental chemistry at or around the

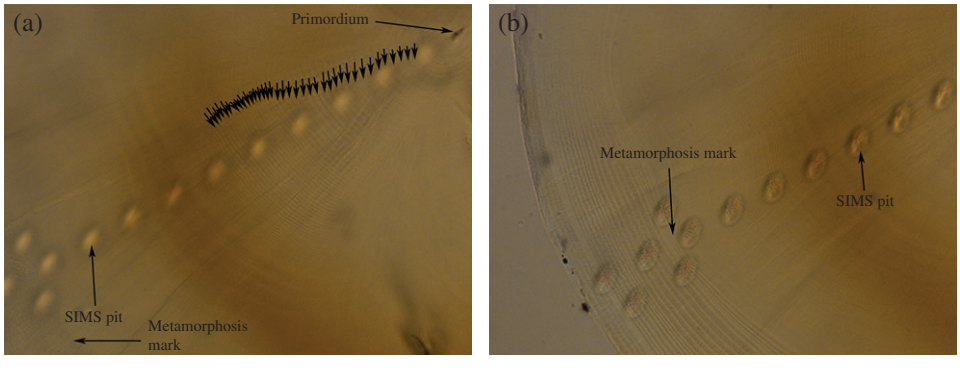

FIG. 2. Example of an *Awaous stamineus* otolith, sampled by SIMS (sample 11543), demonstrating that (a) growth increments (▮) are largest near the primordium (ELG) and increment widths decline during the late larval period (LLG) and (b) growth increment widths are small just prior to the metamorphic mark and then increase following the metamorphic mark. Both images have a field of view of 248·5 μm.

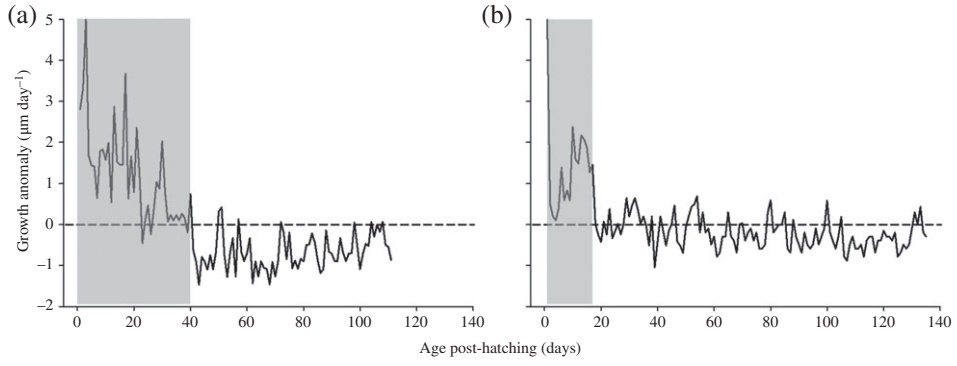

FIG. 3. Larval growth anomalies for *Awaous stamineus* otoliths: (a) sample 10918 from Lawa'i, representing the longest in the dataset and (b) sample 10910 from Lawa'i, Kaua'i the shortest duration anomaly. ▭, Early larval growth period; – – –, the mean larval growth rate (MLG) across the entire larval period. Early larval growth anomalies were defined as growth rates sustained for >3 consecutive days above the MLG.

metamorphosis mark in all individuals (Fig. 5). Sr:Ca ratios were high in the larval period and declined dramatically around the metamorphosis mark, indicating a change from a higher salinity environment (larval Sr:Ca mean = 14·53 mmol mol^{-1}) to a lower salinity environment (post-larval Sr:Ca mean = 5·76 mmol mol^{-1}; Fig. 5). Values of δ^{18}O also shifted downward at metamorphosis by 4–5‰, indicating an abrupt change from a marine to freshwater environment (Fig. 5). In all cases, the δ^{18}O shift occurred precisely at the metamorphosis mark, but the shift in Sr:Ca was less consistent, with some otoliths exhibiting a shift around

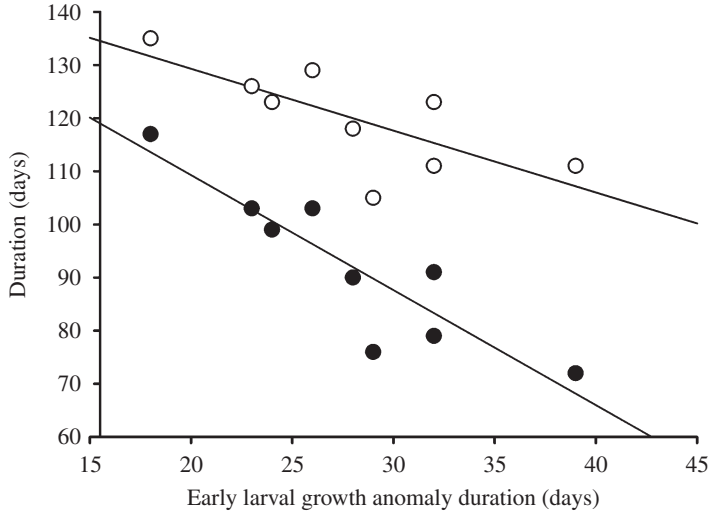

FIG. 4. Correlation (——, the best fit regression lines) between *Awaous stamineus* early larval growth anomaly duration and both late larval duration (●, $y = -2{\cdot}16x + 152{\cdot}17$, $r^2 = 0{\cdot}80$, $P < 0{\cdot}01$) and total pelagic larval duration (○, $y = -1{\cdot}16x + 152{\cdot}17$, $r^2 = 0{\cdot}54$, $P < 0{\cdot}05$).

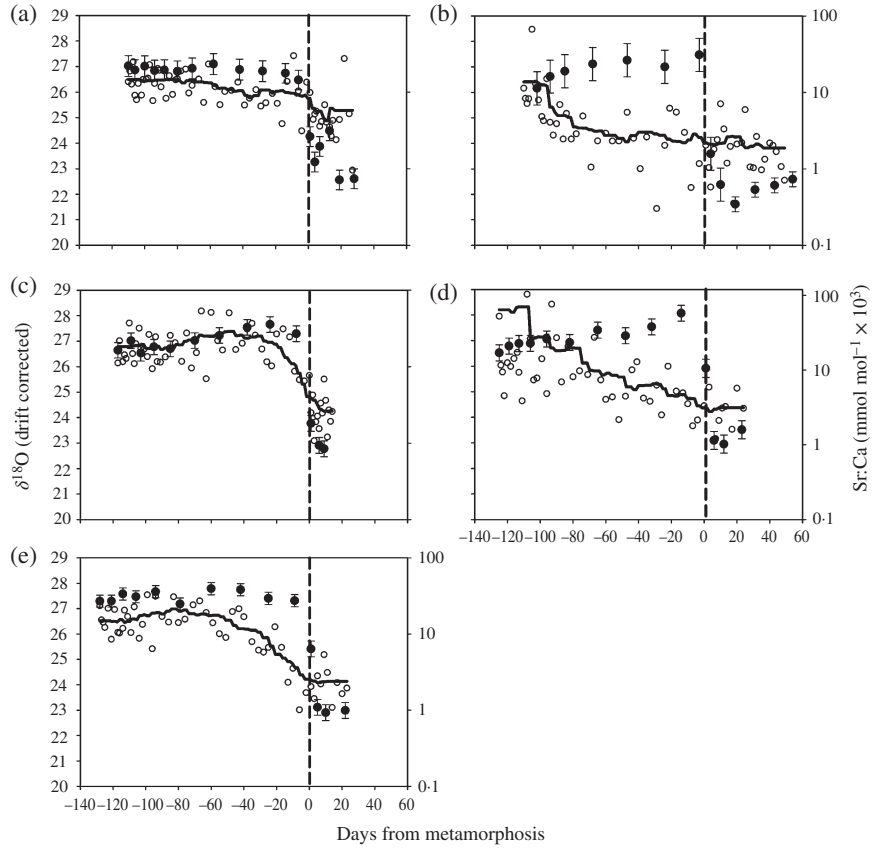

FIG. 5. Otolith transect profiles of mean (±S.D.) δ^{18}O (●) and Sr:Ca (○) for five *Awaous stamineus* (a) sample 10918 from Lawa'i, Kaua'i; (b) sample 11455 from Waimanalo, O'ahu; (c) sample 11542 from Waimea, O'ahu; (d) sample 11543 from Waimea, O'ahu; (e) sample 11527 from Kaluanui, O'ahu. Chemistry profiles are centred around the metamorphosis mark (|).

the metamorphosis mark (*e.g.* 11452, 11527 and 10918) and others demonstrating shifts in Sr:Ca well before the metamorphosis mark (*e.g.* 11455 and 11453; Fig. 5).

Values of δ^{18}O were highly stable from hatching to metamorphosis, often varying less than the precision of the SIMS measurement (±0·3‰) and never varying more than ± 1‰. Multivariate analysis of variance also showed no significant difference in multi-element signatures between the ELG and LLG (MANOVA: $F_{7,10} = 1{\cdot}39$, $P > 0{\cdot}05$, $n = 9$). Interestingly, however, trace element ratios within the ELG were correlated with ELG duration across individuals. A larva with a long ELG period had lower Sr:Ca compared with a counterpart with a short ELG period ($r = -0{\cdot}74$, $P < 0{\cdot}05$, $n = 9$; Fig. 6). Zn:Ca was also correlated with ELG duration ($r = -0{\cdot}68$, $P < 0{\cdot}05$), but visual assessment of the trend suggests that the relationship is driven by two outlier points. Variation in δ^{18}O was not correlated with ELG duration across the sampled individuals.

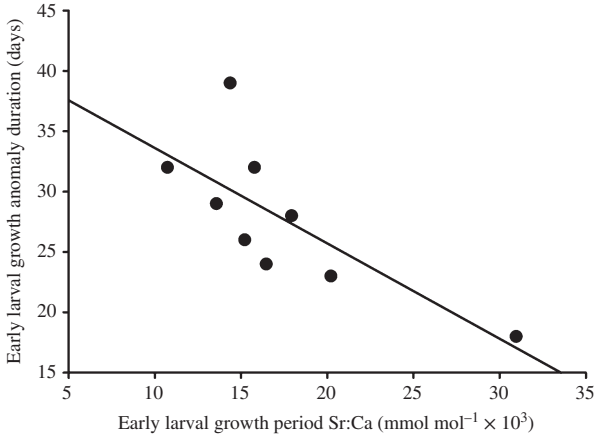

FIG. 6. Correlation between Sr:Ca in the early larval growth periods and the duration of the early larval growth anomaly of *Awaous stamineus*: $y = -0{\cdot}74x + 37{\cdot}04$, $r^2 = 0{\cdot}56$, $P < 0{\cdot}05$.

During the post-larval period, both trace-element chemistry and δ^{18}O varied considerably within individuals occupying stream habitat. Some trace elements varied widely within streams during the post-larval period (*e.g.* Pb; C.V. = 4·79), while others, such as Sr, were more stable (C.V. = 0·18). Values of δ^{18}O varied by as much as 2‰ (C.V. = 0·07) during the post-larval period, indicating that the freshwater stream environment is relatively variable in chemistry and temperature compared with the marine environment. Both trace elements and δ^{18}O also appear to vary among catchments, although trace elements were more variable (C.V. range: 0·47–1·33) than δ^{18}O, which varied by *c.* 1·3‰ (C.V. = 0·02). Interestingly, the only catchment (Waimea, O'ahu) for which δ^{18}O measurements were available from two individuals showed consistency between individuals, the averages differing by only 0·05‰, suggesting that δ^{18}O is a very precise measure of the environment. Post-larval δ^{18}O values, however, were not correlated with stream water temperature at the time of sample collection (slope = −0·22, $r = -0{\cdot}38$, $P > 0{\cdot}05$, $n = 5$).

DISCUSSION

This study illustrates the insights into habitat use and individual growth during early life that can be derived from combining high-resolution data from microstructural and microchemical analyses of fish otoliths. While the sample size is small, the findings show that integrated analysis of daily rings can provide detailed information about differences in growth rates within and between individual fish that are likely to influence survival and fitness. Coupling growth data with environmental inferences from trace element (LA-ICP-MS) and oxygen isotope (SIMS) analyses enabled linking of individual growth with habitat use and environmental conditions. LA-ICP-MS elucidated relationships between environmental chemistry and larval growth, whereas δ^{18}O measurements pinpointed major environmental transitions associated with changes in growth rates. These insights suggest the possibility that integrating multiple analytical approaches could uncover critical differences in habitat use and consequences thereof

for the growth of individuals in other species and settings (Shima & Swearer, 2009; Hogan *et al.*, 2014).

Although only a small number of individuals were examined, the findings indicate that growth rates of *A. stamineus* are not constant throughout early life. All individuals exhibited a pronounced early period of fast growth as larvae, followed by a slow growth period prior to metamorphosis. Consistent with grown patterns observed by Radtke *et al.* (1988), post-larval growth increments markedly increased in size after metamorphosis. The cause of the rapid increase in growth after metamorphosis is not known, but Radtke *et al.* (1988) hypothesized that it is due to morphological changes in feeding structures and a complete shift in diet from marine planktivory to algal grazing and macroinvertebrate feeding in streams. Gross *et al.* (1988) also hypothesized that diadromous fishes will migrate from marine to fresh water in tropical systems because productivity is higher in tropical fresh waters than tropical marine waters allowing for greater foraging opportunities in tropical fresh waters.

Larval growth rate can profoundly influence the probability of survival in fishes by influencing vulnerability to size-selective predation (Houde, 1997). Here, the duration of the fast growth ELG period varied widely among individuals, which could affect fitness by influencing survival and age at first reproduction (Bailey & Houde, 1989). Fast early larval growth may be favoured by selection because size-selective mortality will decrease and survivorship increase once larvae escape a 'window of vulnerability' by reaching a threshold size after which predation risk is dramatically decreased (Cowan *et al.*, 1996). Consistent with this, individuals with longer periods of fast early larval growth tended to achieve comparable size over a shorter larval duration (Fig. 4). Rapidly achieving a relatively large size is undoubtedly advantageous for small goby larvae in the marine environment (Houde, 1997). To understand whether these enhanced growth rates in the ELG influence settlement or recruitment processes, future work should explore selective mortality processes during the larval stage.

Owing to the intimate linkage between mortality and growth arising from size-selective predation (Werner & Gilliam, 1984), extrinsic factors that influence larval growth rates can strongly affect individual survival. Larval habitat use, for example, has been linked with growth performance and survival in fishes (Hamilton *et al.*, 2008; Shima & Swearer, 2009). Here the duration of the ELG period was negatively correlated with certain trace elements, specifically Sr (Sr:Ca, range: 10·7–30·9 mmol mol^{-1}; Fig. 6), which suggests that maximum growth potential may be habitat dependent. Sr:Ca is indicative of environmental salinity (Zimmerman, 2005), whereas higher Sr:Ca ratios generally reflect higher salinity conditions. Thus, the inference from these few samples is that having a shorter ELG period is associated with occupying a fully marine habitat. Even individuals with the longest ELG periods, however, do not exhibit the low Sr:Ca ratios (mean = 5·6 mmol mol^{-1}) characteristic of freshwater streams, which suggests that these individuals reside in estuarine or nearshore environments such as river plumes where salinity is reduced (Sorenson & Hobson, 2005; Hogan *et al.*, 2014). More work will be required to confirm these inferences.

Both trace element chemistry and δ^{18}O records captured transitions from marine or estuarine environments to freshwater environments, but shifts in δ^{18}O were also exactly coincident with the large and clearly visible region on the otolith that has been inferred to mark the metamorphosis of *A. stamineus* larvae into post-larvae. Although

otolith Sr and δ^{18}O have long been used to describe diadromous fish migrations (Casselman, 1982; Nelson *et al.*, 1989), this is the first study to compare high-resolution analyses of both tracers from the same fish. Sr:Ca and δ^{18}O showed marked declines in all samples, providing parallel yet independent evidence of a shift from high to low salinity conditions. SIMS analyses of δ^{18}O, however, identified the point of habitat transition more consistently than LA-ICP-MS analyses of Sr:Ca, which is the most widely used method (Fig. 5). Indeed, the coincidence of larval metamorphosis with the transition to fresh water has only been assumed or approximated in most previous studies (except see Hale & Swearer, 2008), but the high spatial resolution of the SIMS ion beam enabled the precise linking of shifts in larval habitat use with metamorphosis. LA-ICP-MS recovered parallel trends, but some records identified a decline in Sr:Ca prior to the metamorphosis mark (*e.g.* 11453 and 11455; Fig. 5). Freshwater *et al.* (2015) observed the same pattern in migrating sockeye salmon *Oncorhynchus nerka* (Walbaum 1792); some Sr:Ca profiles aligned with the mark while others preceded it. Freshwater *et al.* (2015) suggest that the precedence of chemical signatures relative to visual marks could reflect fish moving into estuaries with high salinity and long salinity gradients. This is not likely in Hawai'ian streams, which typically have a small (or no) estuary with sharp salinity gradients. Instead, it is hypothesized that the difference could be a result of decoupling between the timing of the laser reaching the metamorphic mark and the entry of the resulting ions into the ICP-MS detector, but this seems unlikely to apply to only a sub-set of otoliths. Alternatively, the analysis of a continuous transect by LA-ICP-MS could create some overlap of signals across adjacent growth rings that inevitably blurs sharp chemical transitions compared with the spot-based approach implemented in SIMS. Even if spot sampling was conducted with the LA-ICP-MS, beam width and depth precision are coarse (25 μm width, 10–30 μm depth; Pisonero *et al.*, 2009) compared with SIMS (15 μm × 1 μm). Freshwater *et al.* (2015) also considered this as an alternative explanation for patterns observed in *O. nerka*.

One of the original objectives for examining δ^{18}O variation was to infer environmental temperatures experienced during early life stages. The fractionation of oxygen isotopes between aragonite and water has a predictable equilibrium relationship with temperature (Thorrold *et al.*, 1997; Kim *et al.*, 2007). As a result, a 0·22‰ increase in δ^{18}O (aragonite) is indicative of a 1° C increase in temperature if the δ^{18}O of the water itself is constant (Kim *et al.*, 2007). Interestingly, no relationship was found between δ^{18}O of post-larval otolith material and stream temperatures measured at the time fish were sampled. This is probably a consequence of small sample sizes and point observations of field temperatures that are not necessarily representative of average stream temperature conditions. Additionally, Hawai'ian streams are known to exhibit considerable variability in δ^{18}O (Coplen & Kendall, 2000) owing to differences in precipitation and groundwater sources (Scholl *et al.*, 1996). In contrast, the δ^{18}O measurements from the two post-larvae otolith domains sampled from the same catchment showed remarkable consistency, differing by only 0·05‰, or roughly 0·25° C assuming that δ^{18}O of the water is constant (Table I). This finding suggests that δ^{18}O could be a useful index of environmental temperatures if end-members, including direct δ^{18}O measurements of stream water, were thoroughly sampled to derive correction coefficients (Matta *et al.*, 2013).

Present comparisons indicate that *in situ* δ^{18}O measurements by SIMS seem to be a more powerful tool than trace-element measurements by LA-ICP-MS as δ^{18}O is a more

powerful and versatile proxy for marine–freshwater transitions. SIMS offers significant analytical advantages over LA-ICP-MS of fish otoliths and that it can be a powerful tool for understanding relationships between the environment and fish growth, particularly if end-member chemistry is well constrained. Preparation time, however, analysis cost and equipment access are, at present, major constraints for SIMS. Sample preparation for SIMS requires additional steps (*i.e.* otolith roasting) as well as far greater attention to sample state *i.e.* narrow tolerance of surface flatness and smoothness (Kita *et al.*, 2009) than is required for LA-ICP-MS analysis. The most striking difference between SIMS and LA-ICP-MS is the cost of instrument time and sample throughput. The cost of data collection using SIMS can be significantly higher than LA-ICP-MS. Additionally, SIMS throughput is typically much lower than LA-ICP-MS. For this study, *c.* 12 otolith transects h^{-1} were sampled with LA-ICP-MS, compared with a single otolith transect every *c.* 2 h with SIMS. Thus, on a per-otolith basis, SIMS is much more expensive than LA-ICP-MS. A reduction in the number of SIMS spots per otolith would make the per sample expense more similar to LA-ICP-MS. Given that the $\delta^{18}O$ of the oceanic larval period did not vary much, the number of spots before the metamorphic mark could be reduced without loss of information. The number of SIMS spots, however, would have to be determined experimentally for any given fish species based on the goals of the study.

Although logistical and cost constraints can be challenging, the present results show that parallel analyses of otolith microstructure, microchemistry and $\delta^{18}O$ is a powerful approach for relating environmental history to individual growth in fishes. Using SIMS alongside LA-ICP-MS provided new insight into larval migration and habitat use, especially when combined with microstructural analysis of daily growth and metamorphosis. Even the modest number of samples in this study provided informative results and provides a basis for understanding relationships between habitat use, environmental variability and the growth performance of individual larvae. Each of these factors is known to influence individual survival and has long-term implications for population dynamics. Integrated approaches may also prove useful for reconstructing responses to environmental change, where parallel analyses could track shifts in precipitation or temperature alongside corresponding shifts in fish life history and growth (Rankin & Sponaugle, 2011). The present initial work with Hawai‘ian gobies provides an example of such inferences, illustrating the value of coupled analyses of otolith microstructure and microchemistry in future studies (Starrs *et al.*, 2016).

We thank T. Haas, E. Childress, E. Hain, B. Lamphere, R. Walter and R. Gagne for field assistance; B. Hess, J. Kern and M. Spicuzza for assistance with otolith preparation for SIMS; N. Kita, T. Ushikubo and D. Nakashima for assistance in the WiscSIMS lab; R. Hannigan for LA-ICP-MS facilities and assistance at the University of Massachusetts-Boston; J. Fournelle and P. Gopon for SEM imaging for SIMS preparation at the University of Wisconsin, Madison. Funding was provided by the U.S. Department of Defense Strategic Environmental Research and Development Program under project RC-1646. WiscSIMS is partially supported by NSF-EAR-1053466 and NSF-EAR-1355590.

Supporting Information

Supporting Information may be found in the online version of this paper:

Fig. S1. Scanning electron micrograph image of otolith sample 11543 including the transect of SIMS pits from core to edge. Daily growth bands are visible near the edge of the otolith.

Fig. S2. Scanning electron micrograph image of otolith sample 11543 including a close up view of pits from SIMS analysis. Daily otolith growth bands are visible.
Table SI. Raw data for all analyses undertaken during the study of *Awaous stamineus* otolith microstructure and growth.

References

Bailey, K. M. & Houde, E. D. (1989). Predation on eggs and larvae of marine fishes and the recruitment problem. *Advances in Marine Biology* **25,** 1–83.

Barber, M. C. & Jenkins, G. P. (2001). Differential effects of food and temperature lead to decoupling of short-term otolith and somatic growth rates in juvenile King George whiting. *Journal of Fish Biology* **58,** 1320–1330.

Baumann, H., Wells, R. J. D., Rooker, J. R., Zhang, S., Baumann, Z., Madigan, D. J., Dewar, H., Snodgrass, O. E. & Fisher, N. S. (2015). Combining otolith microstructure and trace elemental analyses to infer the arrival of juvenile Pacific bluefin tuna in the California current ecosystem. *ICES Journal of Marine Science* **72,** 2128–2138.

Ben-Tzvi, O., Abelson, A., Gaines, S. D., Sheehy, M. S., Paradis, G. L. & Kiflawi, M. (2007). The inclusion of sub-detection limit LA-ICPMS data, in the analysis of otolith microchemistry, by use of palindrome sequence analysis (PaSA). *Limnology and Oceanography: Methods* **5,** 97–105.

Bradley, R. S. (1999). *Paleoclimatology*. San Diego, CA: Academic Press, Harcourt Brace and Company.

Brasher, A. M. D. (2003). Impacts of human disturbances in biotic communities in Hawai'ian streams. *BioScience* **53,** 1052–1060.

Campana, S. E. (1999). Chemistry and composition of fish otoliths: pathways, mechanisms and applications. *Marine Ecology Progress Series* **188,** 263–297.

Casselman, J. M. (1982). Chemical analysis of the optically different zones in eel otoliths. In *Proceedings of the 1980 North American Eel Conference* (Loftus, K. H., ed), pp. 74–82. Toronto: Ministry of Natural Resources, Canada.

Cowan, J. H., Houde, E. D. & Rose, K. A. (1996). Size-dependent vulnerability of marine fish larvae to predation: an individual based numerical experiment. *ICES Journal of Marine Science* **53,** 23–37.

Durrant, S. F. & Ward, N. I. (2005). Recent biological and environmental applications of laser ablation inductively coupled plasma mass spectrometry (LA-ICP-MS). *Journal of Analytical Atomic Spectrometry* **20,** 821–829.

Elsdon, T. S., Wells, B. K., Campana, S. E., Gillanders, B. M., Jones, C. M., Limburg, K. E., Secor, D. H., Thorold, S. R. & Walther, B. (2008). Otolith chemistry to describe movements and life history parameters of fishes: hypotheses, assumptions, limitations and inferences. *Oceanography and Marine Biology – An Annual Review* **46,** 297–330.

Freshwater, C., Trudel, M., Beacham, T. D., Neville, C.-E., Tucker, S. & Juanes, F. (2015). Validation of daily increments and a marine-entry check in the otoliths of sockeye salmon *Oncorhynchus nerka* post-smolts. *Journal of Fish Biology* **87,** 169–178.

Grorud-Colvert, K. & Sponaugle, S. (2011). Variability in water temperature affects trait-mediated survival of a newly settled coral reef fish. *Oecologia* **165,** 675–686.

Gross, M. R., Coleman, R. M. & McDowall, R. M. (1988). Aquatic productivity and the evolution of diadromous fish migration. *Science* **239,** 1291–1293.

Ha, P. Y. & Kinzie, R. A. (1996). Reproductive biology of *Awaous guamensis*, an amphidromous Hawai'ian goby. *Environmental Biology of Fishes* **45,** 383–396.

Hale, R. & Swearer, S. E. (2008). Otolith microstructural and microchemical changes associated with settlement in the diadromous fish *Galaxias maculatus*. *Marine Ecology Progress Series* **352,** 229–234.

Hamilton, S. L., Regetz, J. & Warner, R. R. (2008). Post settlement survival linked to larval life in a marine fish. *Proceedings of the National Academy of Sciences* **105,** 1561–1566.

Hogan, J. D., McIntyre, P. B., Blum, M. J., Gilliam, J. F. & Bickford, N. (2014). Consequences of alternative dispersal strategies in a putatively amphidromous fish. *Ecology* **95,** 2397–2408.

Houde, E. D. (1997). Patterns and trends in larval-stage growth and mortality of teleost fish. *Journal of Fish Biology* **51** (Suppl. A), 52–83.
Keith, P. (2003). Biology and ecology of amphidromous Gobiidae of the Indo-Pacific and the Caribbean regions. *Journal of Fish Biology* **63,** 831–847.
Kim, S.-T., O'Neil, J. R., Hillaire-Marcel, C. & Mucci, A. (2007). Oxygen isotope fractionation between synthetic aragonite and water: influence of temperature and Mg2+ concentration. *Geochimica et Cosmochimica Acta* **71,** 4704–4715.
Kita, N. T., Ushikubo, T., Fu, B. & Valley, J. W. (2009). High precision SIMS oxygen isotope analysis and the effect of sample topography. *Chemical Geology* **264,** 43–57.
Kozdon, R., Ushikubo, T., Kita, N. T., Spicuzza, M. & Valley, J. W. (2009). Intratest oxygen isotope variability in the planktonic foraminifer *N. pachyderma*: real *vs*. apparent vital effects by ion microprobe. *Chemical Geology* **258,** 327–337.
Limberg, K. E., Hayden, T. A., Pine, W. E. III, Yard, M. D., Kozdon, R. & Valley, J. W. (2013). Of travertine and time: otolith chemistry and microstructure detect provenance and demography of endangered humpback chub in Grand Canyon, USA. *PLoS One* **8,** e84235.
Lindstrom, D. P., Blum, M. J., Walter, R. P., Gagne, R. B. & Gilliam, J. F. (2012). Molecular and morphological evidence of distinct evolutionary lineages of *Awaous guamensis* in Hawai'i and Guam. *Copeia* **2012,** 293–300.
Matta, M. E., Orland, I. J., Ushikubo, T., Helser, T. E., Black, B. A. & Valley, J. W. (2013). Otolith oxygen isotopes measured by high-precision secondary ion mass spectrometry reflect life history of a yellowfin sole (*Limanda aspera*). *Rapid Communications in Mass Spectrometry* **27,** 691–699.
McDowall, R. M. (2007). On amphidromy, a distinct form of diadromy in aquatic organisms. *Fish and Fisheries* **8,** 1–13.
Mora, C. & Sale, P. F. (2002). Are populations of coral reef fish open or closed? *Trends in Ecology & Evolution* **17,** 422–428.
Nelson, C. S., Northcote, T. G. & Hendy, C. H. (1989). Potential use of oxygen and carbon isotopic composition of otoliths to identify migratory and non-migratory stocks of the New Zealand common smelt: a pilot study. *New Zealand Journal of Marine and Freshwater Research* **23,** 337–344.
Pisonero, J., Fernandez, B. & Gunther, D. (2009). Critical revision of GD-MS, LA-ICP-MS and SIMS as inorganic mass spectrometric techniques for direct solid analysis. *Journal of Analytical Atomic Spectrometry* **24,** 1145–1160.
Radtke, R. L., Kinzie, R. A. & Folsom, S. D. (1988). Age at recruitment of Hawai'ian freshwater gobies. *Environmental Biology of Fishes* **23,** 205–213.
Rankin, T. L. & Sponaugle, S. (2011). Temperature influences selective mortality during the early life stages of a coral reef fish. *PLoS One* **6,** e16814. doi: 10.1371/journal.pone.0016814
Scholl, M. A., Ingebritsen, S. E., Janik, C. J. & Kauahikaua, J. P. (1996). Use of precipitation and groundwater isotopes to interpret regional hydrology in a tropical volcanic island: Kilauea volcano area, Hawai'i. *Water Resources Research* **32,** 3525–3537.
Shima, J. S. & Swearer, S. E. (2009). Larval quality is shaped by matrix effects: implications for connectivity in a marine metapopulation. *Ecology* **90,** 1255–1267.
Sorenson, P. W. & Hobson, K. A. (2005). Stable isotope analysis of amphidromous Hawai'ian gobies suggests their larvae spend a substantial period of time in freshwater river plumes. *Environmental Biology of Fishes* **74,** 31–42.
Starrs, D., Ebner, B. C. & Fulton, C. J. (2016). All in the ears: unlocking the early life history biology and spatial ecology of fishes. *Biological Reviews* **91,** 86–105.
Thorrold, S. R., Campana, S. E., Jones, C. M. & Swart, P. K. (1997). Factors determining $\delta^{13}C$ and $\delta^{18}O$ fractionation in aragonitic otoliths of marine fish. *Geochimica et Cosmochimica Acta* **61,** 2909–2919.
Valley, J. W. & Kita, N. T. (2009). *In situ* oxygen isotope geochemistry by ion microprobe. In *MAC Short Course* (Fayek, M., ed.), pp. 19–63. *Secondary Ion Mass Spectrometry in the Earth Sciences* **41**.
Walter, R. P., Hogan, J. D., Blum, M. J., Gagne, R. B., Hain, E. F., Gilliam, J. F. & McIntyre, P. B. (2012). Climate change and conservation of endemic amphidromous fishes in Hawai'ian streams. *Endangered Species Research* **16,** 261–272.

Weidel, B. C., Ushikubo, T., Carpenter, S. R., Kita, N. T., Cole, J. J., Kitchell, J. F., Pace, M. L. & Valley, J. W. (2007). Diary of a bluegill (*Lepomis macrochirus*): daily $\delta^{13}C$ and $\delta^{18}O$ records in otoliths by ion microprobe. *Canadian Journal of Fisheries and Aquatic Sciences* **64,** 1641–1645.

Weiss, S. B., White, R. R., Murphy, D. D. & Ehrlich, P. R. (1987). Growth and dispersal of the larvae of the checkerspot butterfly *Euphydryas ethida*. *Oikos* **50,** 161–166.

Werner, E. E. & Gilliam, J. F. (1984). The ontogenetic niche and species interactions in size-structured populations. *Annual Review of Ecology and Systematics* **15,** 393–425.

Zimmerman, C. E. (2005). Relationship of otolith strontium-to-calcium ratios and salinity: experimental validation for juvenile salmonids. *Canadian Journal of Fisheries and Aquatic Sciences* **62,** 88–97.

Electronic References

Coplen, T. B. & Kendall, C. (2000). Stable hydrogen and oxygen isotope ratios for selected sites of the U.S. Geological Survey's NASQAN and benchmark surface water networks. *USGS Open-File Report 00-160*. Reston, VA. Available at http://pubs.usgs.gov/of/2000/ofr00-160/pdf/ofr00-160.pdf/

Kinzie, R. A. (1990). Life histories and environmental requirements of coastal vertebrates and invertebrates Pacific Ocean region: amphidromous macrofauna of Hawai'ian island streams. *Technical Report EL-89-10*. Washington, D.C.: Department of the Army. Available at www.dtic.mil/dtic/tr/fulltext/u2/a229842.pdf